Applied Physics Letters

Transition volumes from multiply twinned particles to single crystals of supported Ag and Au nanoparticles

Cite as: Appl. Phys. Lett. **121**, 061604 (2022); https://doi.org/10.1063/5.0100156
Submitted: 21 May 2022 • Accepted: 26 July 2022 • Published Online: 10 August 2022

Peiyu Chen, Fabien Silly, Yingrui Zhao, et al.

Applied Physics Letters ARTICLE scitation.org/journal/apl

Transition volumes from multiply twinned particles to single crystals of supported Ag and Au nanoparticles

Cite as: Appl. Phys. Lett. **121**, 061604 (2022); doi: 10.1063/5.0100156
Submitted: 21 May 2022 · Accepted: 26 July 2022 ·
Published Online: 10 August 2022

Peiyu Chen,[1,a)] Fabien Silly,[1,2] Yingrui Zhao,[1] and Martin R. Castell[1,a)]

AFFILIATIONS

[1]Department of Materials, University of Oxford, Parks Road, Oxford OX1 3PH, United Kingdom
[2]CEA, CNRS, SPEC, TITANS, Université Paris-Saclay, F-91191 Gif sur Yvette, France

[a)]**Authors to whom correspondence should be addressed:** peiyu.chen@materials.ox.ac.uk and martin.castell@materials.ox.ac.uk

ABSTRACT

Shape changes of Ag and Au nanoparticles supported on single crystal reconstructed $SrTiO_3$(001) and (111) substrates were investigated using scanning tunneling microscopy. Both metals nucleate as multiply twinned particles (MTPs) and transform into face-centered-cubic single crystals (SCs) beyond a critical volume. On $SrTiO_3$(001)-$c(4 \times 2)$ the critical volumes are measured as $141 \pm 51\,nm^3$ for Ag and $107 \pm 23\,nm^3$ for Au, whereas on $SrTiO_3$(111)–(4×4)+(6×6) the critical volumes are $53 \pm 26\,nm^3$ for Ag and $26 \pm 40\,nm^3$ for Au. A much larger transition volume was observed on $SrTiO_3$(001)–(2×1), where Ag remains as MTPs up to $3400\,nm^3$, while Au nucleates as atomic monolayers instead of MTPs. This work demonstrates the significant impact of small variations of the surface structure of the substrate on the MTP–SC transition volume.

Studies of noble metal nanoparticles are a significant research topic because of their applications in chemical sensing and catalysis. The ability to control the shape of the nanoparticles is important with respect to optimizing their properties for specific applications. For example, Ag nanoparticles are used in sensing devices that make use of surface-enhanced Raman scattering (SERS),[1,2] and Au nanoparticles can be used as catalysts for carbon monoxide oxidation.[3,4] Different crystal facets of the nanoparticles have been reported to exhibit distinct optical responses[5,6] and catalytic behavior.[7–9] For example, for Au particles, calculations indicate that adsorption and dissociation of O_2 are most efficient on {001} facets.[7] Also, multiply twinned particles (MTPs) of Au and Ag show enhanced optical and electrochemical performance when compared to their spherical counterparts.[10,11] Hence, the particle shape has a large influence on the performance of the material.

MTPs have been comprehensively studied as "modified Wulff shapes."[12–17] Depending on the metal, MTP morphologies are thermodynamically more stable at smaller sizes than their single-crystal (SC) counterparts.[14,17–21] This is because MTPs adopt icosahedral or decahedral shapes that only expose low energy {111} surface facets, although the "Marks decahedron" also contains {001} facets when γ_{001} is sufficiently small such that $\gamma_{111}/\gamma_{001} > 2/\sqrt{3}$.[21] The creation of MTPs incurs the energetic cost of bulk strain and twinning,[22–24] which means that beyond a critical volume, the SC form is thermodynamically more stable. The value of the critical volume depends on the relative surface energies of the {111} and {001} facets, the bulk elastic modulus, the surface stress, and the twinning energy.

The stable sizes of MTPs and their conversion into SCs have been reported in some studies. An interesting example is that icosahedral Pb MTPs were observed to survive up to a relatively large height of 95 nm on a Si(111) substrate.[25] In the case of Ag nanocrystals grown on a rough SiO_2 surface, the energetically equivalent size between decahedral MTPs and face-centered-cubic (fcc) SCs is theoretically predicted to be 11 000 atoms (ca. 8 nm average dimension).[26] For Cu nanocrystals supported on a $SrTiO_3$(001)–(2×1) substrate, the transition size from icosahedral MTPs to fcc SCs was experimentally determined to be ~8500 atoms.[27]

Conversely, theoretical studies show that in their freestanding forms, Cu icosahedral MTPs are only stable at small volumes up to ~1000 atoms, followed by decahedral MTPs up to ~40 000 atoms and finally fcc SCs above this volume.[20] The supporting substrate appears to play an important role in the equilibrium of MTPs vs SCs, though the thermodynamics of the MTP–SC transition is rarely studied in the supported form.[28] Here, we investigate Ag and Au nanocrystals grown on $SrTiO_3$ single crystal substrates by scanning tunneling microscopy (STM).

We prepared two different surfaces of $SrTiO_3$ and show on both substrates how Ag and Au nucleate as icosahedral MTPs and transform into fcc SCs beyond their critical volumes.

Nb-doped $SrTiO_3$ is used as the substrate because it is a good electrically conducting model system for metal-on-oxide growth. $SrTiO_3$ is a cubic oxide with a lattice parameter similar to many metals, and on which it is straightforward to prepare stable (001), (110), and (111) terminations. This enables epitaxial growth of SC metal nanocrystals and investigation of the effects of the different terminations on the SC shapes. It is also possible to change the reconstructions of $SrTiO_3$ surfaces, which provides a further element of surface structure tuning.

Nb-doped $SrTiO_3$ single crystal substrates (0.5 wt. % Nb) were epi-polished on the (001) and (111) surfaces and supplied by PI-KEM, UK. Two surfaces were prepared for Ag and Au growth. To generate the $SrTiO_3(001)$-$c(4 \times 2)$ surface, $SrTiO_3(001)$ was sputtered by Ar^+ ions at 500 eV for 10 min, followed by annealing at 1100–1150 °C for 30 min in ultrahigh vacuum (UHV).[29,30] $SrTiO_3(111)$–(4×4) $+(6 \times 6)$ was generated by Ar^+-ion sputtering at 500 eV for 6 min and subsequent UHV annealing at 1090 °C for 1.5–3 h.[31] Ag was deposited onto the $SrTiO_3$ substrates from an *e*-beam evaporator (Oxford Applied Research EGN4) using 99.95% pure Ag rods supplied by Goodfellow, UK. The samples were held at 25–350 °C during deposition, all followed by post annealing at 350 °C for 1–2 h. Au was deposited onto the substrates using a Createc Knudsen cell heated to 1350 °C. The samples were held at 300–400 °C during deposition. Ag and Au nanoparticles were imaged by STM (JEOL JSTM 4500s model, base pressure 10^{-8} Pa). STM images were processed by Gwyddion, WSxM,[32] FabViewer,[33] and Smart Align.[34,35]

Both Ag and Au adopt an fcc crystal structure in the bulk. The thermodynamically stable shape of their freestanding SCs is predicted by the Wulff construction[36] to be a truncated octahedron [Fig. 1(a)], which has {111} and {001} facets. The MTP shape observed in our study for both metals is an icosahedron [Fig. 1(b)]. It is composed of 20 regular tetrahedra meeting at a central point, exposing 20 {111} facets which are all equilateral triangles. The individual tetrahedra only have {111} facets (the lowest-energy termination), but together they create many internal twin boundaries.

Ag nanocrystals grow as a mixture of MTPs and SCs on both $SrTiO_3(001)$-$c(4 \times 2)$ and $SrTiO_3(111)$–(4×4)+(6×6) substrates. Figure 1(c) shows an STM image of Ag nanocrystals supported on the $SrTiO_3(001)$-$c(4 \times 2)$ surface. In this image, most Ag nanocrystals are icosahedral MTPs, and a small proportion are fcc SCs (indicated by white arrows). Figures 1(d) and 1(e) show close-up images of fcc SCs of Ag with two different orientations. Most SCs adopt a truncated triangular shape with (111) top and base facets [Fig. 1(d)]. The supported MTPs are observed to adopt three high-symmetry orientations named the point, face, and edge orientations,[37,38] as shown in Figs. 1(f)–1(h), respectively.

Similar investigations were carried out for Au nanoparticles on $SrTiO_3(001)$-$c(4 \times 2)$ and $SrTiO_3(111)$–(4×4)+(6×6) substrates. Figure 2(a) shows Au nanoparticles grown on $SrTiO_3(111)$–(4×4) $+(6 \times 6)$, which are a mixture of icosahedral MTPs and fcc SCs (indicated by white arrows). All observed SCs adopt the truncated hexagonal shape [Fig. 2(b)] on both substrates. The three observed orientations of MTPs (point, face, and edge) are magnified in Figs. 2(c)–2(e).

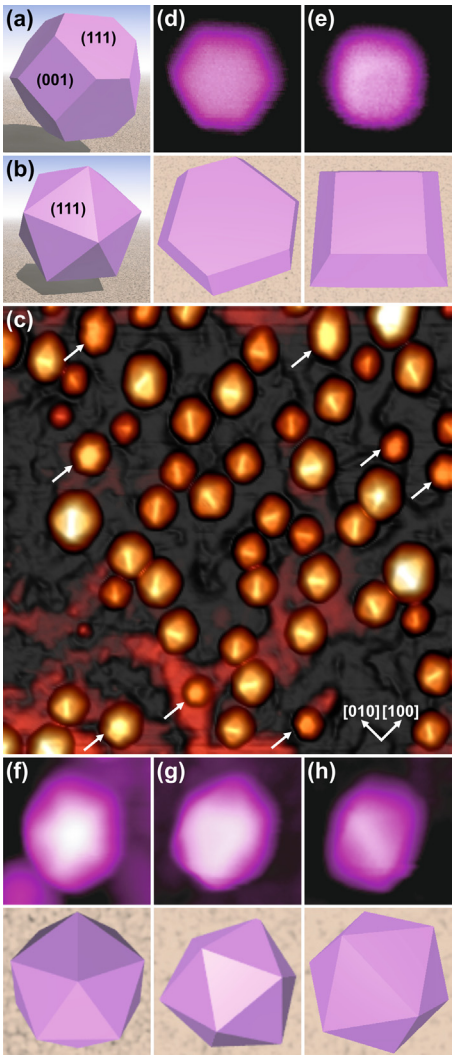

FIG. 1. Ag nanocrystals on $SrTiO_3$ substrates. (a) and (b) 3D models of (a) a freestanding fcc SC and (b) a freestanding icosahedral MTP. (c) STM image showing a mixture of MTPs and SCs on $SrTiO_3(001)$-$c(4 \times 2)$. The SCs are indicated by white arrows. (d) and (e) Magnified STM images (top) and models (bottom) of Ag SCs with (d) a truncated triangular shape and (e) a truncated pyramidal shape. (f)–(h) Magnified STM images (top) and models (bottom) of Ag MTPs with (f) point, (g) face, and (h) edge orientations. Image sizes: (c) $100 \times 100\,nm^2$, (d) $13 \times 13\,nm^2$, (e) $10 \times 10\,nm^2$, and (f)–(h) $14 \times 14\,nm^2$; scanning parameters for all images: $V_s = 4.0$ V, $I_t = 0.03$ nA.

Before presenting our quantitative analysis, we point out that most crystals are well-equilibrated, which was assisted by annealing at $\geq$ 300 °C. For example, SCs with truncated triangular top facets are mostly threefold rotationally symmetric; MTPs with the point orientation are fivefold rotationally symmetric. Particles that do not satisfy these conditions are excluded from the measurement statistics. The annealing temperatures of 300–400 °C give rise to particle ripening, which, together with the deposition amounts of the metals, ensures a suitable size distribution of particles containing a good mixture of MTPs and SCs, enabling us to study the MTP–SC transition size.

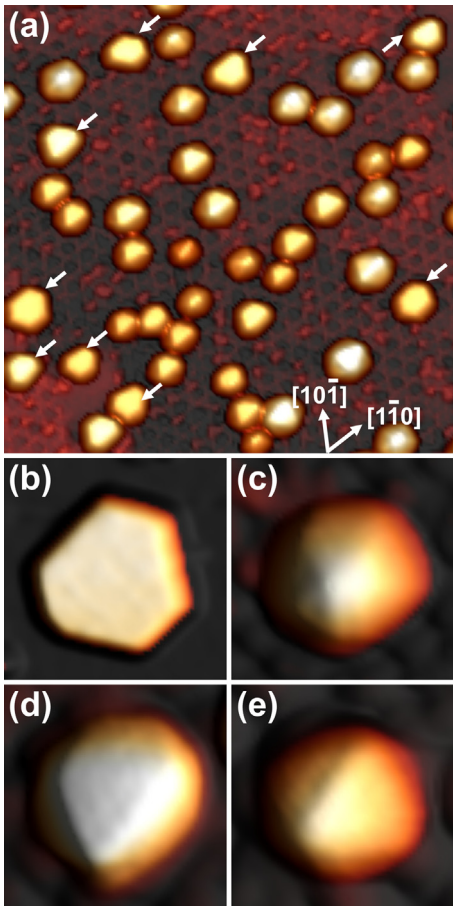

FIG. 2. Au nanocrystals on $SrTiO_3$ substrates. (a) STM image showing a mixture of icosahedral MTPs and fcc SCs on $SrTiO_3(111)$–(4×4)+(6×6). The SCs are indicated by white arrows. (b)–(e) Magnified STM images of (b) an SC and MTPs with (c) point, (d) face, and (e) edge orientations. Image sizes: (a) $63 \times 63\,nm^2$, (b) $38 \times 38\,nm^2$, and (c)–(e) $8 \times 8\,nm^2$; scanning parameters: (a) $V_s = 4.0\,V$, $I_t = 0.10\,nA$, (b) $V_s = 1.0\,V$, $I_t = 0.05\,nA$, and (c)–(e) $V_s = 4.0\,V$, $I_t = 0.05\,nA$.

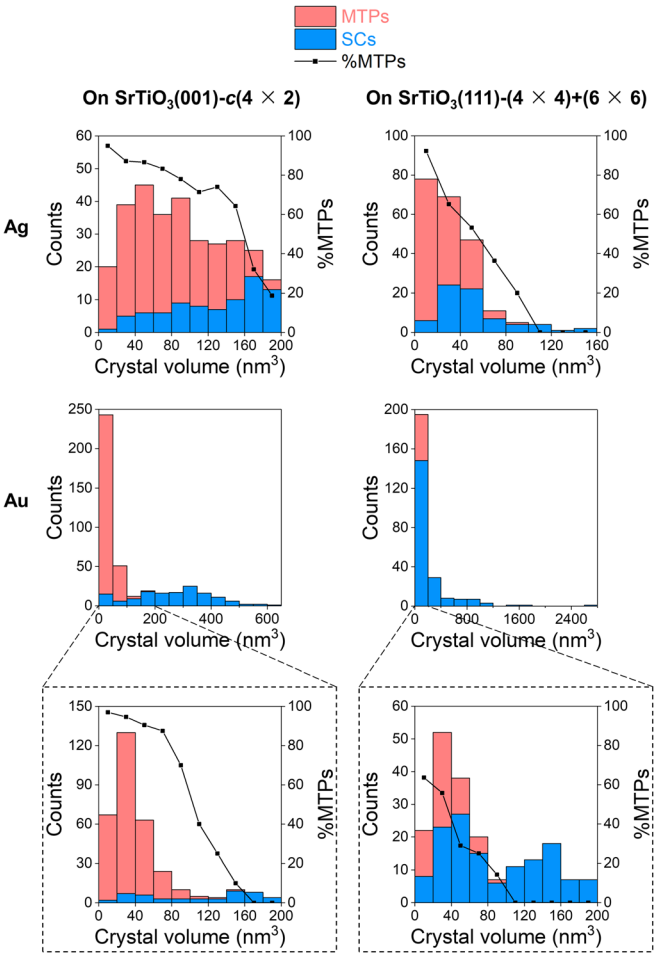

FIG. 3. Populations of Ag (first row) and Au (second and third rows) MTPs and SCs at different crystal volumes on $SrTiO_3(001)$-$c(4 \times 2)$ and $SrTiO_3(111)$–(4×4) + (6×6).

Example measurements of dimensions (Fig. S1), equations used for volume calculations, and more source images (Figs. S2–S16) are supplied in the supplementary material.

The histograms in Fig. 3 show the populations of MTPs and SCs of Ag (first row) and Au (second and third rows) as a function of crystal volume on the two $SrTiO_3$ substrates. For Au nanocrystals (second row), MTPs are only observed at sizes $< 200\,nm^3$ on both substrates, so the statistics for crystals $< 200\,nm^3$ are magnified in the third row. On both substrates and for both metals, the decreasing proportion of MTPs with increasing size confirms that MTPs are the energetically favorable shape in the small-size regime.

To analyze the transition from MTPs to SCs for both metals, let us define the transition size as the volume at which a crystal has the same probability of adopting an MTP and an SC form, i.e., 50%. Table I summarizes the transition sizes of Ag and Au MTPs supported on three different $SrTiO_3$ substrates. The data on $SrTiO_3(001)$–(2×1) are included for comparison from our previous reports.[37–39] The error associated with each number denotes the standard deviation of the measurement distribution.

On both $SrTiO_3(001)$-$c(4 \times 2)$ and $SrTiO_3(111)$–(4×4)+(6×6) substrates, the transition volume of Ag MTPs is found to be at least 30% greater than for Au. The thermodynamic stabilities of MTPs and SCs depend on the following factors in order of relative importance:[21] (i) facet energies γ_{111} and γ_{001} > (ii) bulk strain energy[17,40] > (iii) surface stress energy[41] > (iv) twin boundary energy. Below, we discuss how these factors may have given rise to the observed differences between Ag and Au. (i) The facet energy ratio $\gamma_{111}/\gamma_{001}$ is 0.95 ± 0.03 for Ag and 0.88 ± 0.07 for Au (based on the γ_{111} and γ_{001} values in Patra *et al.*'s report).[42] The fact that $\gamma_{111}/\gamma_{001} < 1$ for both metals confirms that they are both more stable in the MTP form if only the facet energies are being considered. The exact value of $\gamma_{111}/\gamma_{001}$ does not influence the MTP–SC transition size because it is already taken care of by the area ratio of the {111}/{001} facets when the particles are in the SC form. (ii) The elastic bulk modulus of Ag (100 GPa) is substantially lower than that of Au (180 GPa). The lower the bulk modulus, the less elastic energy is

TABLE I. Transition sizes (50% MTPs + 50% SCs) of Ag and Au nanocrystals supported on $SrTiO_3$ substrates. The errors denote the standard deviations of the measured shape distributions.

	$SrTiO_3(001)$-$c(4\times2)$	$SrTiO_3(111)$–(4×4)+(6×6)	$SrTiO_3(001)$–(2×1)
Ag	$141\pm51\ nm^3$ (8300 ± 3000 atoms)	$53\pm26\ nm^3$ (3100 ± 1500 atoms)	$>3400\ nm^3$ (> 200 000 atoms)[37]
Au	$107\pm23\ nm^3$ (6300 ± 1400 atoms)	$26\pm40\ nm^3$ (1500 ± 2400 atoms)	Au monolayers observed instead of MTPs[38,39]

required to keep the particles in the MTP form, thus stabilizing Ag MTPs to larger sizes. Note that the angle between the {111} twins is 70.52°, and that for a fivefold symmetric particle, there is a missing 7.40° closing angle ($360^\circ - 5\times70.52^\circ = 7.40^\circ$), so the strain for the Au and Ag MTPs is the same, but the elastic energy in the Au MTPs is larger. (iii) The effect of surface stress on the relative stabilities of icosahedral and decahedral MTPs and SCs has been thoroughly discussed by Patala *et al.*[41] It has been discovered that a larger MTP (icosahedral)–SC transition size is achieved when the surface stress factor is higher, though exact values have not been proposed for Ag and Au in UHV. (iv) Finally, the twin boundary energy of Ag (10.0 mJ m^{-2}) is almost half that of Au (17.5 mJ m^{-2}),[17] which also helps to stabilize Ag MTPs to larger sizes.

In addition to the factors discussed above, for supported MTPs, the MTP–SC transition size is also influenced by γ^* ($=\gamma_i-\gamma_s$), i.e., the difference between the crystal–substrate interfacial energy and the substrate surface energy.[43] Our experimental results reveal the significant effect of the supporting substrate: in our previous report of Ag nanocrystals on $SrTiO_3(001)$–(2×1), only MTPs but no SCs were observed, up to a volume of ~200 000 atoms.[37] In the current study, however, the transition size for Ag crystals is found to be 8300 ± 3000 atoms on $SrTiO_3(001)$-$c(4\times2)$ and 3100 ± 1500 atoms on $SrTiO_3(111)$–$(4\times4)+(6\times6)$, i.e., more than 20 times smaller.

One factor that possibly helps to stabilize Ag MTPs on $SrTiO_3(001)$–(2×1) is that its substrate surface energy is significantly higher than the other two by 0.4–0.6 J m^{-2}.[44–46] Such a high substrate surface energy encourages a greater degree of wetting of the supported metal particles, i.e., a flatter aspect ratio. Additionally, $SrTiO_3(001)$–(2×1) is special amongst all $SrTiO_3$ reconstructed surfaces because it is the only known hydroxylated surface.[44] Being terminated with –OH groups, it may result in a chemical environment that is different from the other reconstructions. However, the exact mechanism remains inconclusive without information on the interfacial structure, which requires further study. The high surface energy of $SrTiO_3(001)$–(2×1) has an even greater effect on supported Au islands: no MTPs are observed at all but instead the nucleation shape is a 2D Au monolayer, as reported previously.[38,39] These monolayers also convert into SCs at larger sizes.

Finally, we note that for both Ag and Au MTPs, the transition size is a few times greater on $SrTiO_3(001)$-$c(4\times2)$ than on $SrTiO_3(111)$–$(4\times4)+(6\times6)$. This consistency possibly suggests a higher substrate surface energy γ_s for $SrTiO_3(001)$-$c(4\times2)$ than for $SrTiO_3(111)$–$(4\times4)+(6\times6)$. Another explanation is that since most Ag and Au SCs have (111) base facets, $SrTiO_3$ substrates with a (111) termination should result in a lower interfacial energy γ_i due to better epitaxy, thereby encouraging an earlier transition to the SC form compared with a (001) substrate. For both possibilities above, γ^* ($=\gamma_i-\gamma_s$) is the critical parameter in determining the MTP–SC transition size.

In summary, STM investigation of Ag and Au crystal growth on $SrTiO_3(001)$-$c(4\times2)$, $SrTiO_3(111)$–$(4\times4)+(6\times6)$, and $SrTiO_3(001)$–(2×1) reveals that not only the nucleation shapes of Ag and Au particles are affected by the supporting $SrTiO_3$ substrates, but also their transition sizes into SCs. The MTP–SC transition size is found to be larger on a higher-energy substrate, and it is also larger for Ag than for Au. Hence, this study demonstrates the potential to manipulate crystal morphology via substrate engineering, e.g., promoting the growth of a given facet or shape (MTP/SC) that is the most optically interesting for SERS applications or the most active for catalytic applications.

See the supplementary material for example measurements of dimensions, equations used for volume calculations, and more source images.

This work was supported by the Engineering and Physical Sciences Research Council (UK) under Grant No. EP/M015173/1. The authors would also like to thank the Royal Society and Defence Science and Technology Laboratory (Dstl) for funding and Mr. Chris Spencer (JEOL UK) for valuable technical support.

AUTHOR DECLARATIONS

Conflict of Interest

The authors have no conflicts to disclose.

Author Contributions

Peiyu Chen: Conceptualization (equal); Data curation (equal); Formal analysis (equal); Investigation (equal); Methodology (equal); Project administration (equal); Resources (equal); Software (equal); Validation (equal); Visualization (equal); Writing – original draft (equal); Writing – review and editing (equal). **Fabien Silly:** Conceptualization (equal); Data curation (equal); Formal analysis (supporting); Methodology (equal); Resources (supporting); Software (supporting); Visualization (equal); Writing – review and editing (supporting). **Yingrui Zhao:** Data curation (supporting); Investigation (supporting); Methodology (supporting). **Martin R. Castell:** Conceptualization (equal); Formal analysis (equal); Funding acquisition (equal); Investigation (equal); Project administration (equal); Resources (equal); Supervision (equal); Validation (equal); Writing – review and editing (equal).

DATA AVAILABILITY

The data that support the findings of this study are available within the article and its supplementary material.

REFERENCES

[1]X. Qiu, J. Gu, T. Yang, C. Ma, L. Li, Y. Wu, C. Zhu, H. Gao, Z. Yang, Z. Wang, X. Li, A. Hu, J. Xu, L. Zhong, J. Shen, A. Huang, and G. Chen, Spectrochim. Acta, Part A **276**, 121212 (2022).

[2]D. Wang, L. Bao, H. Li, X. Guo, W. Liu, X. Wang, X. Hou, and B. He, Nanoscale **14**, 6212 (2022).
[3]R. Camposeco and R. Zanella, Catal. Today **392–393**, 49 (2022).
[4]H. Yang, J. Cen, Q. Wu, C. J. Ridge, X. Tong, C. Zhou, V. Veerasamy, D. Su, C. M. Lindsay, M. Liu, and A. Orlov, J. Phys. Chem. C **126**, 4836 (2022).
[5]N. Macia, R. Bresoli-Obach, S. Nonell, and B. Heyne, J. Am. Chem. Soc. **141**, 684–692 (2019).
[6]Á. I. López-Lorente, Anal. Chim. Acta **1168**, 338474 (2021).
[7]M. Boronat and A. Corma, Dalton Trans. **39**, 8538 (2010).
[8]B. Shen, L. Huang, J. Shen, K. He, C. Y. Zheng, V. P. Dravid, C. Wolverton, and C. A. Mirkin, Proc. Natl. Acad. Sci. **118**, e2105722118 (2021).
[9]M. Liu, B. A. Lu, G. Yang, P. Yuan, H. Xia, Y. Wang, K. Guo, S. Zhao, J. Liu, Y. Yu, W. Yan, C. L. Dong, J. N. Zhang, and S. Mu, Adv. Sci. **9**, 2200147 (2022).
[10]Z. X. Xie, W. C. Tzeng, and C. L. Huang, ChemPhysChem **17**, 2551 (2016).
[11]M. Xu, L. Zhang, and F. Zhao, ACS Appl. Mater. Interfaces **12**, 12186 (2020).
[12]S. Ino and S. Ogawa, J. Phys. Soc. Jpn. **22**, 1365 (1967).
[13]L. D. Marks, J. Cryst. Growth **61**, 556–566 (1983).
[14]L. D. Marks, Philos. Mag. A **49**, 81 (1984).
[15]H. Hofmeister, Z. Fur Krist. **224**, 528 (2009).
[16]E. Ringe, R. P. Van Duyne, and L. D. Marks, J. Phys. Chem. C **117**, 15859–15870 (2013).
[17]A. Howie and L. D. Marks, Philos. Mag. A **49**, 95 (1984).
[18]C. L. Cleveland and U. Landman, J. Chem. Phys. **94**, 7376 (1991).
[19]M. J. Yacamán, J. A. Ascencio, H. B. Liu, and J. Gardea-Torresdey, J. Vac. Sci. Technol. B **19**, 1091 (2001).
[20]C. Mottet, J. Goniakowski, F. Baletto, R. Ferrando, and G. Treglia, Phase Transitions **77**, 101 (2004).
[21]L. D. Marks and L. Peng, J. Phys.: Condens. Matter **28**, 53001 (2016).
[22]D. Seo, C. I. Yoo, I. S. Chung, S. M. Park, S. Ryu, and H. Song, J. Phys. Chem. C **112**, 2469 (2008).
[23]C. Lofton and W. Sigmund, Adv. Funct. Mater. **15**, 1197 (2005).
[24]J. L. Elechiguerra, J. Reyes-Gasga, and M. J. Yacaman, J. Mater. Chem. **16**, 3906 (2006).
[25]L. Serrier-Garcia, F. Debontridder, D. Demaille, T. Cren, and D. Roditchev, J. Phys. Chem. C **119**, 12651 (2015).
[26]K. D. Gilroy, J. Puibasset, M. Vara, and Y. Xia, Angew. Chem. Int. Ed. **56**, 8647 (2017).
[27]F. Silly and M. R. Castell, ACS Nano **3**, 901 (2009).
[28]Z. R. Mansley and L. D. Marks, J. Phys. Chem. C **124**, 28038 (2020).
[29]M. R. Castell, Surf. Sci. **505**, 1–13 (2002).
[30]M. R. Castell, Surf. Sci. **516**, 33 (2002).
[31]B. C. Russell and M. R. Castell, J. Phys. Chem. C **112**, 6538 (2008).
[32]I. Horcas, R. Fernández, J. M. Gómez-Rodríguez, J. Colchero, J. Gómez-Herrero, and A. M. Baro, Rev. Sci. Instrum. **78**, 013705 (2007).
[33]F. Silly, J. Microsc. **236**, 211 (2009).
[34]L. Jones, S. Wang, X. Hu, S. ur Rahman, and M. R. Castell, Adv. Struct. Chem. Imaging. **4**, 7 (2018).
[35]L. Jones, H. Yang, T. J. Pennycook, M. S. J. Marshall, S. Van Aert, N. D. Browning, M. R. Castell, and P. D. Nellist, Adv. Struct. Chem. Imaging **1**, 8 (2015).
[36]G. Wulff, Z. Kristallogr. Cryst. Mater. **34**, 449 (1901).
[37]F. Silly and M. R. Castell, Appl. Phys. Lett. **87**, 213107 (2005).
[38]F. Silly and M. R. Castell, Phys. Rev. Lett. **96**, 086104 (2006).
[39]P. Chen, K. Murugappan, and M. R. Castell, Phys. Chem. Chem. Phys. **22**, 4416 (2020).
[40]S. Patala, L. D. Marks, and M. Olvera De La Cruz, J. Phys. Chem. C **117**, 1485–1494 (2013).
[41]S. Patala, L. D. Marks, and M. Olvera De La Cruz, J. Phys. Chem. Lett. **4**, 3089–3094 (2013).
[42]A. Patra, J. E. Bates, J. Sun, and J. P. Perdew, Proc. Natl. Acad. Sci. **114**, E9188 (2017).
[43]W. L. Winterbottom, Acta Metall. **15**, 303 (1967).
[44]A. E. Becerra-Toledo, M. R. Castell, and L. D. Marks, Surf. Sci. **606**, 762 (2012).
[45]F. Silly and M. R. Castell, Phys. Rev. Lett. **94**, 046103 (2005).
[46]O. Warschkow, M. Asta, N. Erdman, K. R. Poeppelmeier, D. E. Ellis, and L. D. Marks, Surf. Sci. **573**, 446 (2004).